Ca^{2+} Dependence of the Distance between Cys-98 of Troponin C and Cys-133 of Troponin I in the Ternary Troponin Complex. Resonance Energy Transfer Measurements†

Terence Tao,* Elizabeth Gowell, Gale M. Strasburg,‡ John Gergely, and Paul C. Leavis

Department of Muscle Research, Boston Biomedical Research Institute, Department of Neurology, Harvard Medical School, and Department of Biological Chemistry and Molecular Pharmacology, Harvard Medical School, Boston, Massachusetts 02114

Received October 11, 1988; Revised Manuscript Received February 28, 1989

ABSTRACT: We have used resonance energy transfer to study the spatial relationship between Cys-98 of rabbit skeletal troponin C and Cys-133 of rabbit skeletal troponin I in the reconstituted ternary troponin complex. The donor was introduced by labeling either troponin C or troponin I with *N*-(iodoacetyl)-*N'*-(5-sulfo-1-naphthyl)ethylenediamine, while the acceptor was introduced by labeling either protein with *N*-[4-(dimethylamino)phenyl-4'-azophenyl]maleimide. The extent of energy transfer was determined by measuring the quenching of the donor fluorescence decay. The results indicate first that the distance between these two sites is not fixed, suggesting that the protein regions involved possess considerable segmental flexibility. Second, the mean distance between the two sites is dependent on the metal-binding state of troponin C, being 39.1 Å when none of the metal-binding sites are occupied, 41.0 Å when Mg^{2+} ions bind at the high-affinity sites, and 35.5 Å when Ca^{2+} ions bind to the low-affinity sites. Neither the magnitude of the distances nor the trend of change with metal ions differs greatly when the locations of the probes are switched or when steady-state fluorometry was used to determine the transfer efficiency. Since the low-affinity sites have been implicated as the physiological triggering sites, our findings suggest that one of the key events in Ca^{2+} activation of skeletal muscle contraction is a ~5-Å decrease in the distance between the Cys-98 region of troponin C and the Cys-133 region of troponin I.

Contraction of mammalian striated muscle is regulated by Ca^{2+}, a process that requires the regulatory proteins troponin (Tn)[1] and tropomyosin (Tm) (Ebashi & Endo, 1968). Tn is composed of three subunits, the Ca^{2+}-binding, the inhibitory, and the Tm-binding subunits (TnC, TnI, and TnT, respectively). TnC has two classes of metal-binding sites, the high-affinity Ca^{2+}/Mg^{2+} sites (sites III and IV) and the low-affinity Ca^{2+}-specific sites (sites I and II) (Potter & Gergely, 1975); the latter sites are thought to be the physiologically Ca^{2+}-triggering sites (Johnson et al., 1979; Robertson et al., 1981). TnI by itself inhibits the Mg^{2+}-ATPase activity of actomyosin (Hartshorne & Mueller, 1968; Schaub & Perry, 1969; Greaser & Gergely, 1971; Perry et al., 1972) and binds to both actin and Tm–actin (Potter & Gergely, 1974; Hitchcock, 1975). TnC neutralizes the inhibition of actomyosin ATPase by TnI both in the presence and in the absence of Ca^{2+} (Perry et al., 1972; Weeks & Perry, 1978). TnC dissociates TnI from Tm–actin in the presence but not in the absence of Ca^{2+} (Potter & Gergely, 1974; Hitchcock, 1975). Full Ca^{2+}-dependent regulation of actomyosin ATPase is only achieved when all three subunits are added to Tm–actin (Greaser & Gergely, 1971).

Numerous studies have characterized the interactions between the thin filament proteins to deduce how the Ca^{2+}-triggering signal is propagated from TnC to the rest of the thin filament [reviewed by Leavis and Gergely (1984) and Zot and Potter (1987)]. Particularly important are the interactions between TnC and TnI, since it is plausible that the regulatory signal is first transmitted to TnI and then to the other proteins in the thin filament. There is considerable evidence that the region in rabbit skeletal TnC containing its sole sulfhydryl, Cys-98, interacts with TnI (Grabarek et al., 1981; Chong & Hodges, 1981; Dalgarno et al., 1982; Leavis et al., 1984; Leszyk et al., 1987).

In this work, we used the technique of resonance energy transfer to measure the distance between probes attached at Cys-98 of TnC and Cys-133 of TnI in the reconstituted ternary Tn complex. We found first that this distance is not fixed, indicating some flexibility on the part either of the protein regions involved or of the attached probes. Second, the mean distance varies depending on the occupancy of the metal-binding sites in TnC, it being 39.1 Å in the absence of any bound metal ion, 41.0 Å when the high-affinity sites are occupied by Mg^{2+}, and 35.5 Å when both the high- and the low-affinity sites are occupied by Ca^{2+}. These results indicate that binding of Ca^{2+} to TnC causes a decrease in the distance

†Supported by grants from the National Institutes of Health (AR21673 to T.T., HL20464 to P.C.L., R37-HL05949 to J.G., and BRSG RR05711) and the Muscular Dystrophy Association (to P.C.L. and J.G.). Presented in part and in preliminary form at the Biophysical Discussions, 1985 (Tao et al., 1986).

*Address correspondence to this author at the Department of Muscle Research, Boston Biomedical Research Institute, 20 Staniford St., Boston, MA 02114.

‡Present address: Department of Food Science and Human Nutrition, Michigan State University, East Lansing, MI 48824.

[1] Abbreviations: 1,5-IAEDANS, *N*-(iodoacetyl)-*N'*-(5-sulfo-1-naphthyl)ethylenediamine; DAB-Mal, *N*-[4-(dimethylamino)phenyl-4'-azophenyl]maleimide; Hepes, *N*-(2-hydroxyethyl)piperazine-*N'*-2-ethanesulfonic acid; EDTA, ethylenediaminetetraacetate; DTT, dithiothreitol; Tn, troponin; Tm, tropomyosin; TnC, TnI, and TnT, the Ca^{2+}-binding, inhibitory, and Tm-binding subunits of Tn, respectively; S1, myosin subfragment 1; C^d, 1,5-IAEDANS-labeled TnC; C^d–I–T, ternary Tn complex reconstituted with C^d, TnI, and TnT; C^d–I^a–T, Tn reconstituted with C^d, DAB-Mal-labeled TnI, and TnT; C–I^d–T, Tn reconstituted with TnC, 1,5-IAEDANS-labeled TnI, and TnT; C^a–I^d–T, Tn reconstituted with DAB-Mal-labeled TnC, 1,5-IAEDANS-labeled TnI, and TnT.

0006-2960/89/0428-5902$01.50/0

between Cys-98 of TnC and Cys-133 of TnI by ~5 Å. Further, Ca^{2+} titration studies indicate that this distance decrease occurs in response to the binding of Ca^{2+} at the low-affinity sites of TnC. This event may represent an important step in Ca^{2+} regulation of skeletal muscle contraction.

Experimental Procedures

Protein Preparation. Tn, Tn subunits, and Tm were prepared from rabbit skeletal ether powder as described in Greaser and Gergely (1973). Actin was prepared from rabbit skeletal acetone powder according to the method of Spudich and Watt (1971). Myosin was prepared according to the method of Balint et al. (1975). S1 was prepared from myosin according to the method of Weeds and Pope (1977). Reconstitution of Tn was carried out by mixing equimolar amounts of the three subunits in a solution of 6 M urea, 5 mM DTT, and 20 mM Hepes, pH 7.5, and then dialyzing against 0.1 M NaCl, 1 mM $CaCl_2$, 2 mM DTT, and 5 mM Hepes, pH 7.5.

Protein Labeling. Cys-98 on TnC was labeled by using 1,5-IAEDANS (Aldrich) as described in Grabarek et al. (1983) or with DAB-Mal (Molecular Probes, Junction City, OR) by incubating TnC (~20 μM, in 0.1 M NaCl, 1 mM EDTA, and 5 mM Hepes, pH 7.5) with DAB-Mal [~40 μM, added from a 10 mM dimethylformamide (Fisher) stock solution] for 2 h at room temperature. The reaction was quenched with excess DTT and then dialyzed against 0.1 M NaCl and 5 mM Hepes, pH 7.5. Labeling of TnI followed a procedure that has been shown previously to modify only Cys-133 (Chong & Hodges, 1982; Strasburg et al., 1985); reconstituted Tn (~10 μM, in 0.1 M NaCl, 1 mM $CaCl_2$, and 5 mM Hepes, pH 7.5) was incubated with 1,5-IAEDANS or DAB-Mal (molar ratio of 2:1 reagent:protein) for 2 h at room temperature, followed by quenching with excess DTT and dialysis. The labeled TnI was isolated from the other two subunits by DEAE-Sephadex chromatography in the presence of urea (Greaser & Gergely, 1973).

Protein concentrations and extent of labeling were estimated by spectrophotometry using the following A_{280} (1 mg/mL, 1 cm) values: 0.18 for TnC, 0.40 for TnI, 0.50 for TnT, and 0.45 for Tn. For the probes the following extinction coefficients were used: ϵ_{337}(AEDANS) = 6000 M^{-1} cm^{-1}, ϵ_{280}(AEDANS) = 1300 M^{-1} cm^{-1} (Hudson & Weber, 1976), ϵ_{460}(DAB) = 46 000 M^{-1} cm^{-1}, and ϵ_{280}(DAB) = 8500 M^{-1} cm^{-1} (Tao et al., 1983). Typically, the extent of labeling is 1.0 mol/mol for AEDANS-TnC, DAB-TnC, and DAB-TnI and 0.7 mol/mol for AEDANS-TnI, with an experimental error of ~10%.

Spectroscopic Measurements. Steady-state fluorometry was carried out on a Perkin-Elmer/Hitachi MPF-4 spectrofluorometer. Fluorescence decay measurements were carried out on a modified Ortec 9300 nanosecond fluorometer as described previously (Leavis et al., 1984). Analyses by the method of moments (Small & Isenberg, 1976) was carried out on a PDP-11/44 minicomputer. Unless otherwise specified, fluorescence measurements were carried out at 25 °C in a buffer containing 5 mM Hepes and 0.1 M NaCl, pH 7.5, at protein concentrations of 2–5 μM.

To correct for concentration mismatch and trivial absorption, the samples were treated with 6 M urea and 5 mM EDTA to dissociate the complexes and to denature the proteins. The spectra of samples containing acceptor and of those not containing acceptor were then scaled with respect to each other so that the peak intensities of the denatured samples were identical.

Distance Calculations. Transfer efficiencies and distances were calculated from the Föster equations [reviewed by Fairclough and Cantor (1978) and Stryer (1978)]

$$E = 1 - \tau_{da}/\tau_d = 1 - \phi_{da}/\phi_d \quad (1)$$

$$R = R_0(E^{-1} - 1)^{1/6} \quad (2)$$

$$R_0 = [(8.79 \times 10^{-5})\kappa^2 n^{-4} \phi_d J]^{1/6} \text{ (Å)} \quad (3)$$

where ϕ_{da} and ϕ_d are donor quantum yields in the presence and absence of acceptor, respectively, τ_{da} and τ_d are donor lifetimes in the presence and absence of acceptor, respectively, R_0 is the critical transfer distance, κ^2 is the orientation factor, n is the refractive index, and J is the overlap integral between the donor fluorescence and acceptor absorption spectra.

To calculate R_0, κ^2 was taken to be $^2/_3$, an assumption whose validity will be discussed. n was taken to be 1.4, a value that is typical for protein solutions (Fairclough & Cantor, 1978). Since neither the extinction coefficient nor the shape of the absorption spectrum of the DAB moiety changes significantly when attached to different proteins, J was taken to be 5.0158 $\times 10^{14}$ cm^{-1} M^{-1} nm^4, a value previously measured for the AEDANS–DAB couple attached to $\alpha\alpha$Tm and F-actin, respectively (Tao et al., 1983). ϕ_d for AEDANS attached to Cys-98 of TnC was obtained from

$$\phi_d(C^d) = \phi_d(Tm^d)\tau_d(C^d)/\tau_d(Tm^d)$$

where $\phi_d(Tm^d)$ = 0.53 and $\tau_d(Tm^d)$ = 13.5 ns are the fluorescence quantum yield and lifetime, respectively, of the AEDANS moiety attached to $\alpha\alpha$Tm (Tao et al., 1983), and $\tau_d(C^d)$ = 17.5 ns is obtained in this work. $\phi_d(I^d)$ was obtained the same way by taking $\tau_d(I^d)$ to be 14.5 ns, the lifetime of the major decay component for AEDANS-TnI.

The transfer efficiency E was obtained from the steady-state measurements by taking the ratio ϕ_{da}/ϕ_d as the ratio between the peak heights of the normalized fluorescence spectra (Figure 1). To calculated E from the lifetime measurements, τ_d was taken to be τ for C^d–I–T and τ_{da} was taken to be τ for the short-lived components of C^d–I^a–T in cases when the donor is attached to TnC and acceptor attached to TnI. In cases when the donor is attached to TnI and acceptor attached to TnC, τ_d and τ_{da} were taken as τ of the major decay components of C–I^d–T and Ca^a–I^d–T, respectively. Separation distances were then calculated by using eq 2.

The range of values that a distance can take on owing to the uncertainty in the value of κ^2 was estimated as described in Stryer (1978). Defining the factor α as $R/R_{2/3}$, where R is the true distance and $R_{2/3}$ is the distance obtained under the assumption that $\kappa^2 = {}^2/_3$, then

$$[0.75(1 - \langle\cos^2\gamma\rangle_\theta)]^{1/6} \leq \alpha \leq (6\ \langle\cos^2\gamma\rangle_\theta)^{1/6} \quad (4)$$

where

$$\langle\cos^2\gamma\rangle_\theta = \int_0^\theta \cos^2\gamma \sin\gamma\, d\gamma / \int_0^\theta \sin\gamma\, d\gamma = (1 - \cos^3\theta)/3(1 - \cos\theta)$$

where θ, the semiangle of a cone within which the probe can undergo rapid rotational motion, can be obtained from (Kawato et al., 1977)

$$A_1/A_0 = \cos^2\theta(1 + \cos\theta)^2/4$$

where A_0 is the theoretical maximum anisotropy of the probe and A_1 is the observed limiting anisotropy obtained by either steady-state or time-dependent polarization measurements. It should be noted that eq 4 corrects an error in Stryer (1978), in which the equation for α contains $\cos^2\theta$ rather than $\langle\cos^2\gamma\rangle_\theta$ (L. Stryer, private communication).

Table I: ATPase Activities of Myosin S1 in the Presence of Reconstituted Thin Filaments: Effects of TnI and TnC Modifications[a]

sample	ATPase activity[b] (s^{-1}) EGTA	Ca^{2+}
S1 + actin + Tm	0.20	0.20
S1 + actin + Tm + I^a + TnT	0.07	0.07
S1 + actin + Tm + C^d–I^a–T	0.09	0.22
S1 + actin + Tm + native Tn	0.07	0.39

[a] I^a is DAB-labeled TnI; C^d is AEDANS-labeled TnC. [b] Measured under conditions specified in Strasburg et al. (1985), with an estimated uncertainty of 0.01 unit.

Results

Throughout this work, the AEDANS and DAB moieties attached to either Cys-98 or TnC or Cys-133 of TnI were used as the energy-transfer donor and acceptor, respectively. The overlap between the fluorescence spectrum of the AEDANS donor and the absorption spectrum of the DAB acceptor is such that one can expect Förster-type resonance energy transfer to occur when the two probes are separated by ~40 Å (Tao et al., 1983). Both steady-state and lifetime measurements were used to characterize the extent of energy transfer. Four different Tn complexes were prepared: (1) C^d–I–T, donor-labeled TnC complexed with unlabeled TnI and TnT; (2) C^d–I^a–T, donor-labeled TnC complexed with acceptor-labeled TnI and unlabeled TnT; (3) C–I^d–T, donor-labeled TnI complexed with unlabeled TnC and TnT; (4) C^a–I^d–T, donor-labeled TnI complexed with acceptor-labeled TnC and unlabeled TnT. Measurements were carried out on the complexes in three metal-binding states: (1) the Ca^{2+} state in which both the high- and the low-affinity metal-binding sites of TnC are saturated by Ca^{2+}, simulating the in vivo activated state; (2) the Mg^{2+} state in which only the high-affinity sites of TnC are occupied by Mg^{2+}, simulating the in vivo relaxed state; (3) the apo state in which neither class of sites is occupied by metal ions.

Activities of the Labeled Proteins. The ability of the labeled proteins to participate in Ca^{2+}-dependent regulation of actomyosin ATPase activity was investigated. It has been shown previously that TnC labeled at Cys-98 with the AEDANS moiety is effective in Ca^{2+} regulation (Grabarek et al., 1983). Here we find that TnI labeled at Cys-133 with DAB-Mal in the complex with TnT is as effective in inhibiting Tm–actin–S1 ATPase activity as unlabeled Tn in the absence of Ca^{2+} (Table I). The reconstituted C^d–I^a–T complex is still capable of regulating Tm–Actin–S1 ATPase activity in a Ca^{2+}-dependent manner, but it is not as effective as native Tn. These results indicate that modification of either TnC or TnI singly has only small effects on the activities of these proteins. The activity of reconstituted Tn that contains both modified proteins is impaired, but not totally abolished.

Steady-State Fluorescence Measurements. For all three metal-binding states, the fluorescence intensity of C^a–I^d–T is considerably lower than that of C–I^d–T (Figure 1A), indicating that the presence of the TnC-bound acceptor substantially quenches the fluorescence of the TnI-bound donor owing to energy transfer. The extent of donor quenching is higher for the Ca^{2+} state than for the Mg^{2+} and apo states, suggesting that more energy transfer occurs in the presence of Ca^{2+} than in its absence. Similar conclusions are reached when the fluorescence intensity of C^d–I^a–T was compared with that of C^d–I–T (Figure 1B), viz, substantial energy transfer occurs under all metal-binding conditions and more energy transfer occurs in the Ca^{2+} state than in the Mg^{2+} or apo states. These results indicate that regardless of the donor–acceptor locations the probes are closer together in the presence of Ca^{2+} than in its absence.

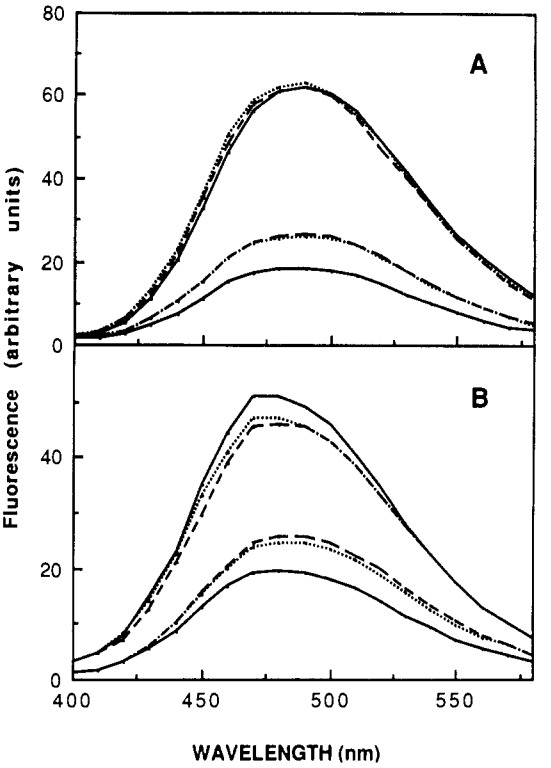

FIGURE 1: Fluorescence spectra (uncorrected) of the AEDANS donor in the absence (upper three curves) and presence (lower three curves) of the DAB acceptor. In panel A the upper spectra are for C–I^d–T and the lower spectra are for C^a–I^d–T. In panel B the upper spectra are for C^d–I–T and the lower spectra are for C^d–I^a–T. Measurements were made in the Ca^{2+} state (0.1 mM $CaCl_2$, solid lines), apo state (0.1 mM $CaCl_2$ and 2 mM EGTA, dotted lines), and Mg^{2+} state (0.1 mM $CaCl_2$, 2 mM EGTA, and 2 mM $MgCl_2$, broken lines). $CaCl_2$, EGTA, and $MgCl_2$ were successively added to the same samples directly into the cuvette. The spectra were scaled to correct for trivial absorbance and concentration mismatch as described under Experimental Procedures.

Table II: Fluorescence Decay Parameters[a]

material	τ_1 (ns)	τ_2 (ns)	τ_3 (ns)	χ^2/N
C–I^d–T (Ca^{2+})[c]		14.38 (0.912)	24.30 (0.088)	13.5
C^a–I^d–T (Ca^{2+})[c]		4.05 (0.701)	16.77 (0.299)	18.6
C–I^d–T (Mg^{2+})[c]		14.92 (0.951)	25.02 (0.049)	15.3
C^a–I^d–T (Mg^{2+})[c]		7.90 (0.632)	17.08 (0.368)	17.6
C–I^d–T (apo)[c]		14.51 (0.902)	23.30 (0.098)	15.6
C^a–I^d–T (apo)[c]		8.07 (0.701)	17.78 (0.299)	11.1
C^d–I–T (Ca^{2+})[b]			17.29 (1.000)	7.2
C^d–I^a–T (Ca^{2+})[c]		4.83 (0.714)	17.95 (0.286)	23.4
C^d–I^a–T (Ca^{2+})[d]	1.22 (0.643)	8.73 (0.195)	18.02 (0.162)	4.5
C^d–I–T (Mg^{2+})[b]			17.71 (1.000)	9.5
C^d–I^a–T (Mg^{2+})[c]		8.45 (0.759)	18.68 (0.241)	21.2
C^d–I^a–T (Mg^{2+})[d]	3.48 (0.243)	9.84 (0.536)	18.17 (0.222)	6.2
C^d–I–T (apo)[b]			18.00 (1.000)	7.3
C^d–I^a–T (apo)[c]		7.43 (0.712)	18.06 (0.288)	16.5
C^d–I^a–T (apo)[d]	3.62 (0.396)	10.69 (0.412)	18.47 (0.192)	6.4

[a–d] Obtained by mono-[b], bi-[c], and triexponential[d] method-of-moments analysis. τ_1, τ_2, and τ_3 are lifetimes of decay components. In parentheses are fractional amplitudes. χ^2/N is the goodness of fit parameter, defined as $(1/N)\sum_{i=1}^{N}(I_{c,i} - I_{e,i})^2/I_{e,i}$, where $I_{c,i}$ and $I_{e,i}$ are calculated and experimental intensities in the ith channel, respectively, and N is the number of channels. See abbreviations footnote and Results for designation of materials and metal-binding states.

Lifetime Measurements. The fluorescence decay of C–I^d–T is adequately described by two exponentials in all three metal-binding states; method-of-moments analysis yielded a major component (~0.9 fractional amplitude) of lifetime τ

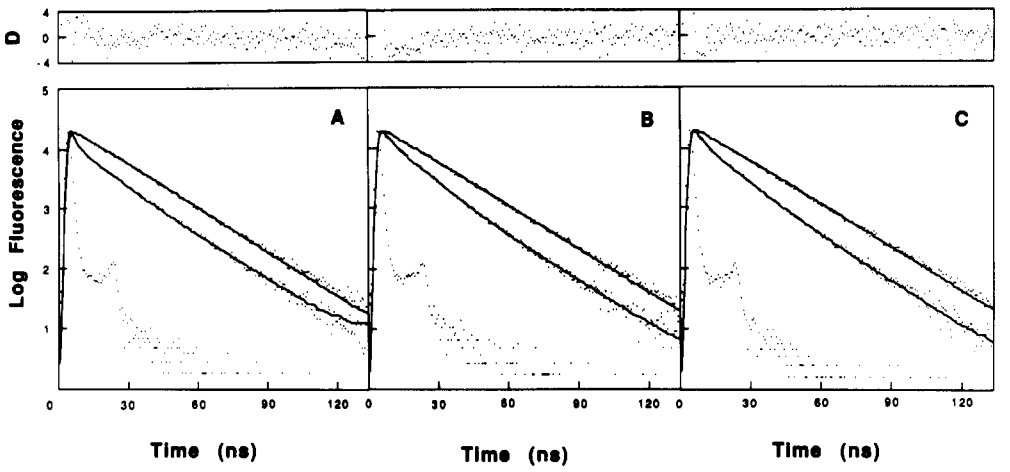

FIGURE 2: Fluorescence decay curves of the AEDANS donor in the absence (C^d–I–T, upper curves) and presence (C^d–I^a–T, lower curves) of the DAB acceptor. Dots are experimental points. Solid lines are calculated fits, obtained with the use of parameters derived from mono- (for C^d–I–T) and tri- (for C^d–I^a–T) exponential method-of-moments analyses (see Table II). Top panels show the difference function, D, for the C^d–I^a–T data; D is defined as $(I_{c,i} - I_{e,i})/(I_{e,i})^{1/2}$, where $I_{c,i}$ and $I_{e,i}$ are calculated and experimental fluorescence intensities, respectively, in the ith channel. The dotted curve at lower left is the excitation curve. Measurements were made on the same samples in the Ca^{2+} (panel A), apo (panel B), and Mg^{2+} (panel C) states as described in the legend for Figure 1.

= 14–15 ns (Table II). For the decay curves of C^a–I^d–T, biexponential analysis yielded lifetimes of 4–8 ns for the major component. Consistent with the steady-state measurements, this lifetime is considerably shorter for the Ca^{2+} state than for the two Ca^{2+}-free states (4 vs 8 ns), indicating that the donor–acceptor separation is smaller in the presence of Ca^{2+} than in its absence.

For all three metal-binding states the fluorescence decay of C^d–I–T is monoexponential (τ = 17–18 ns), while that of C^d–I^a–T is markedly multiexponential (Figure 2, Table II). Bioexponential method-of-moments analyses of the C^d–I^a–T decay curves yielded a long lifetime whose magnitude is comparable to that of C^d–I–T (i.e., the unquenched lifetime) and a short lifetime that is considerably shorter than the unquenched lifetime (5–8 ns). To a first approximation the long-lived component corresponds to TnC-bound donors that are not near any acceptors owing to either incomplete acceptor labeling or partial complex dissociation, while the short-lived comonent corresponds to donors whose excited-state lifetime is decreased by energy transfer to nearby acceptors. As for C^a–I^d–T, the lifetime of the short-lived component is shorter for the Ca^{2+} state than for the Mg^{2+} and apo states (4.8 vs. 8.5 and 7.4 ns, respectively), indicating that the donor–acceptor separation distance is smallest in the Ca^{2+} state.

The C^d–I^a–T decay curves are poorly described by two exponentials, especially for the Ca^{2+} state. Triexponential analysis yielded a long lifetime that is again identical with the unquenched lifetime, an intermediate lifetime, and a short lifetime. These results are interpreted as revealing the presence of multiple donor–acceptor separation distances, and the short and intermediate lifetimes can be used to estimate the range of these distances. The lifetime of the short-lived component is shorter for the Ca^{2+} than for the Mg^{2+} and apo states (1.2 vs 3.5 and 3.6 ns, respectively), indicating that the probes can come closer together in the presence of Ca^{2+} than in its absence. Also, the fractional amplitude of the short-lived component is larger for the Ca^{2+} than for the Mg^{2+} or apo states, indicating that a higher proportion of donors is in close proximity to acceptors in the presence of Ca^{2+} than in its absence.

The data obtained from the steady-state and decay measurements were used to estimate separation distances. As shown in Table III, all the distances are in the range 35–43 Å and are in reasonably good agreement with each other. For each measurement, the distance for the Ca^{2+} state is consistently shorter by ~5 Å than those for the Mg^{2+} or apo states. Distances were also calculated by using lifetimes obtained from triexponential analysis of the C^d–I^a–T data. The significance of these distances will be discussed.

Table III: Distances between Cys-98 of TnC and Cys-133 of TnI Measured by Energy Transfer[a]

material	ϕ_{da}*	ϕ_d*	τ_{da} (ns)	τ_d (ns)	E	R_0 (Å)	R (Å)
C^a–I^d–T (Ca^{2+})[b]	18	62			0.705	40.4	34.9
C^a–I^d–T (Mg^{2+})[b]	27	62			0.571	40.4	38.5
C^a–I^d–T (apo)[b]	26	63			0.589	40.4	38.0
C^a–I^d–T (Ca^{2+})[c]			4.05	14.38	0.718	40.4	34.6
C^a–I^d–T (Mg^{2+})[c]			7.90	14.92	0.471	40.4	41.2
C^a–I^d–T (apo)[c]			8.07	14.51	0.444	40.4	41.9
C^d–I^a–T (Ca^{2+})[b]	19	51			0.620	41.6	38.4
C^d–I^a–T (Mg^{2+})[b]	26	46			0.439	41.6	43.3
C^d–I^a–T (apo)[b]	25	47			0.476	41.6	42.3
C^d–I^a–T (Ca^{2+})[c]			4.83	17.29	0.721	41.6	35.5
C^d–I^a–T (Mg^{2+})[c]			8.45	17.71	0.523	41.6	41.0
C^d–I^a–T (apo)[c]			7.34	18.00	0.592	41.6	39.1
C^d–I^a–T (Ca^{2+})[d]			1.22	17.29	0.929	41.6	27.1
C^d–I^a–T (Mg^{2+})[d]			3.48	17.71	0.804	41.6	32.9
C^d–I^a–T (apo)[d]			3.62	18.00	0.799	41.6	33.1
C^d–I^a–T (Ca^{2+})[e]			8.73	17.29	0.495	41.6	41.7
C^d–I^a–T (Mg^{2+})[e]			9.84	17.71	0.444	41.6	43.2
C^d–I^a–T (apo)[e]			10.69	18.00	0.406	41.6	44.3

[a] ϕ_{da}* and ϕ_d* are relative donor fluorescence yields in the presence and absence of acceptor, respectively; τ_{da} and τ_d are donor lifetimes in the presence and absence of acceptor, respectively; E is the transfer efficiency; R_0 is the critical transfer distance; R is the determined separation distance. [b] ϕ_{da}* and ϕ_d* were obtained from the peak heights of the steady-state fluorescence spectra (Figure 1). [c] τ_{da} was taken to be the lifetime of the major decay component obtained by biexponential analysis. [d] τ_{da} was taken to be the lifetime of the short decay component obtained by triexponential analysis. [e] τ_{da} was taken to be the lifetime of the intermediate decay component obtained by triexponential analysis.

Titration Studies. The dependence of the interprobe distance on metal ions for the C^d–I^a–T complex was further investigated by monitoring the steady-state fluorescence intensity of the C^d–I^a–T complex as a function of Ca^{2+} concentrations. The titration curve is biphasic when Mg^{2+} is absent, with the fluorescence intensity rising in the low Ca^{2+} concentration region and dropping in the high Ca^{2+} concentration range (Figure 3). This indicates that the interprobe distance increases when Ca^{2+} occupies the high-affinity sites

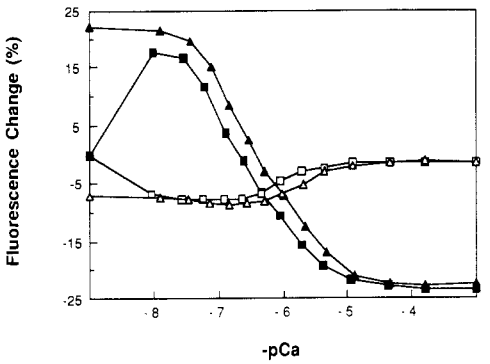

FIGURE 3: Changes in the fluorescence intensity of the AEDANS donor in the absence (C^d–I–T, open symbols) and presence (C^d–I^a–T, solid symbols) of the DAB acceptor as a function of [Ca^{2+}]. Measurements were made in a Ca^{2+}–EGTA buffer system as described in Strasburg et al. (1985), either in the absence (squares) or presence (triangles) of 2 mM $MgCl_2$. The left-most points were obtained in 2 mM EGTA alone (with or without Mg^{2+}). The right-most points were obtained in saturating Ca^{2+}. The ordinate is defined as $(F - F_0)/F_0$, where F is the observed fluorescence intensity, and F_0 is the intensity in the presence of 2 mM EGTA alone. Excitation and emission wavelengths were 337 and 480 nm, respectively.

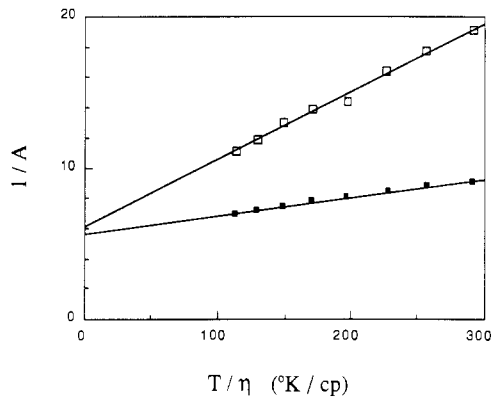

FIGURE 4: Perrin plots of C^d (open squares) and C^d–I–T (solid squares). A is the steady-state anisotropy defined as $(I_\parallel - I_\perp)/(I_\parallel - 2I_\perp)$, where $I_\parallel$ and $I_\perp$ are the parallel and perpendicular components of polarized emission. T is the absolute temperature, and η is the viscosity in centipoise, varied by the addition of sucrose. Measurements were made at 20 °C in the presence of 0.1 mM $CaCl_2$.

and then decreases as the low-affinity sites are occupied. When Mg^{2+} is present, the rising phase in the low Ca^{2+} concentration range is absent. The remaining titration curve is similar to that when Mg^{2+} was absent. For C^d–I–T, the changes in fluorescence intensity as a function of Ca^{2+} concentration are smaller than those for C^d–I^a–T and occur in the opposite direction; i.e., the intensity decreases in the low Ca^{2+} range and increases in the high Ca^{2+} range. They reflect changes in the environment of the label. The presence of Mg^{2+} in the sample abolishes the decrease in intensity in the low-Ca^{2+} range.

Polarization Measurements. Both steady-state and time-dependent fluorescence polarization measurements were carried out on uncomplexed AEDANS–TnC (C^d) and the C^d–I–T complex to measure the limiting anisotropy, A_1, of the AEDANS moiety. As expected, the slope of the steady-state Perrin plot (Figure 4) is larger for C^d–I–T than for C^d owing to the higher molecular mass of the C^d–I–T complex. On the other hand, A_1 of C^d (0.165) and A_1 of C^d–I–T (0.179) are comparable to each other and are considerably smaller than the theoretical maximum of 0.4. These results indicate that in either C^d alone or the ternary C^d–I–T complex the AEDANS probe is considerably depolarized by either rapid rotational motion or intrinsic depolarization processes. Similar

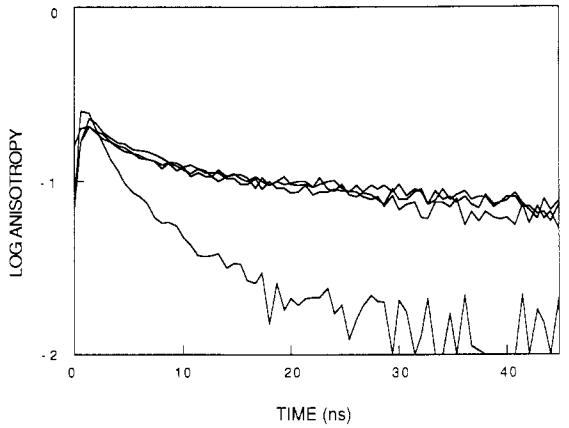

FIGURE 5: Anisotropy decay of C^d in the Ca^{2+} state (lower curve) and of C^d–I–T in the Ca^{2+}, Mg^{2+}, and apo states (upper three overlapping curves). Measurements were made at 20 °C.

results were obtained from anisotropy decay measurements; for C^d alone the anisotropy decays more rapidly than that for C^d–I–T, again consistent with increase in molecular mass when C^d is incorporated into the ternary Tn complex (Figure 5). A_1 for C^d–I–T is similar to that for C^d, in agreement with the steady-state polarization measurements. Neither A_1 nor the shapes of the anisotropy decay curves for C^d–I–T are dependent on metal binding; the former indicates that the rapid depolarization of AEDANS is independent of metal binding, while the latter indicates that the overall shape of the C^d–I–T complex is independent of metal binding.

Discussion

We have used both steady-state and time decay fluorescence measurements to monitor the extent of energy transfer between probes attached to Cys-98 of TnC and Cys-133 of TnI. Regardless of the type of measurement and regardless of whether the donor is on TnC and the acceptor on TnI or vice versa, all the results indicate that the extent of energy transfer is higher in the presence of Ca^{2+} than in its absence, suggesting that the binding of Ca^{2+} to TnC results in a decrease in the distance between the two probe attachment sites. Our Ca^{2+} titration measurements (Figure 3) show that the increase in transfer efficiency (decrease in donor fluorescence) occurs at relatively high Ca^{2+} concentrations (0.1–1 μM) and that the transition is only slightly affected by the presence of Mg^{2+} (which binds only to the high-affinity sites), indicating that the distance decrease occurs in response to binding of Ca^{2+} at the low-affinity sites of TnC, sites that have been implicated as the physiologically relevant triggering sites (Johnson et al., 1979).

Although we have extracted quantitative distance information from all four data sets (Table III), we feel that the data obtained from time decay measurements of samples composed of donor-labeled TnC (C^d–I–T and C^d–I^a–T) yield the most reliable information. This is because the steady-state measurements are subject to errors arising from the inner filter effect, concentration mismatching, and partial complex dissociation. Although the usual procedure was used to correct for the first two errors (described under Experimental Procedures), we could not correct the last one because there is no reliable way to measure the extent of complex dissociation. Although lifetime measurements obviate most of the difficulties encountered in steady-state measurements, the lifetime data obtained from samples composed of donor-labeled TnI (C–I^d–T and C^a–I^d–T) are complex due to the fact that the decay of C–I^d–T is biexponential. This means that the decay of C^a–I^d–T is in principle even more complex. We nevertheless

carried out biexponential analysis on the decay of C^a–I^d–T and used the lifetimes of the major decay components for distance calculations, recognizing the fact that the distance so obtained represents an approximation. We should point out, however, that this approximation is a reasonably good one because the amplitudes of the major components are relatively large and because two exponentials seem to fit the experimental decay curves reasonably well. In contrast, the decay of C^d–I–T is monoexponential with the same lifetimes in all three metal-binding states. As discussed below, this provides the opportunity for the most reliable and detailed analysis of the interprobe proximity relationships.

Whereas the decay of C^d–I–T is monoexponential, that of C^d–I^a–T is considerably more complex. As a first approximation, and to provide a comparison with the C^a–I^d–T data, biexponential analyses were carried out. The analyses yielded a short- and a long-lived component; the lifetime of the latter is identical with that of C^d–I–T. We interpret this decay component to arise from donor moieties that do not undergo any energy transfer due to either incomplete acceptor labeling of TnI or partial dissociation of the acceptor-labeled TnI. We consider the latter to be more likely since the labeling ratio of the DAB-TnI was measured to be 1.0, although the uncertainty of such measurements is at least 10%. The short-lived component would then arise from donor moieties that undergo energy transfer to nearby TnI-bound acceptors. Using the lifetime of this component, we obtained distances of 35, 41, and 39 Å for the Ca^{2+}, Mg^{2+}, and apo states, respectively. We feel that these distances represent some mean interprobe separation distance and note that the magnitudes of these distances as well as the trend with respect to metal binding are consistent with the other data sets.

It is clear, however, that adequate description of the C^d–I^a–T decay curves requires triexponential analyses, which yielded the same long-lived component attributable to donors that do not undergo energy transfer and two additional components whose mere presence indicates some heterogeneity in the interprobe separation distance. For simplicity, we assumed that there are two distances and used the lifetimes of the short and intermediate components to calculate them. As shown in Table III, the two distances are 27 and 42 Å for the Ca^{2+} state; both distances increase (to ~33 and ~44 Å, respectively) for the Mg^{2+} and apo states. We conclude from the above that the distance between Cys-98 of TnC and Cys-133 of TnI is not unique and can be represented by at least two distances. Judging from the smaller of the two distances, the two residues can come rather close to each other, considering that the sizes of the attached probes might sterically prevent a closer mutual approach.

We should point out that, in principle, the interprobe separation may be represented by more than two distances. Indeed, it may be represented by a continuous distribution of distances (Amir & Haas, 1987; Haas et al., 1975; Lakowicz et al., 1988). We have not attempted to analyze our data according to such models because doing so would require an accurate determination of the extent of complex dissociation. Judging from the quality of the fit between the calculated triexponential curves and the experimental curves, we feel that our two-distance model is a reasonable approximation to the actual situation.

Throughout this work we have calculated distances with the assumption that the orientation factor κ^2 can be taken as the isotropically averaged value of $^2/_3$, the validity of which deserves discussion. It has been pointed out by several authors that the choice of $^2/_3$ as κ^2 is not an unreasonable one owing to electronic and rotational depolarization mechanisms (Haas et al., 1978; Stryer, 1978; Perkins et al., 1984; dos Remedios et al., 1987). We have carried out both steady-state and time-dependent depolarization measurements and verified that the initial anisotropy for TnC-bound AEDANS donor is considerably lower than the theoretical maximum of 0.4. Using the formalism presented by Stryer (1978), we have estimated the uncertainty in the distance measurements. Assuming that the acceptor is fixed and the donor can undergo rapid reorientation within a cone, the semiangle θ of this cone was calculated to be 40.5° by using 0.4 as the maximum anisotropy and 0.179 as the initial anisotropy (obtained from steady-state depolarization measurement on C^d–I–T and considered most reliable). The factor α was then calculated to be $0.815 \leq \alpha \leq 1.24$, or an uncertainty in the distances of 19–24%. In practice, this uncertainty should be smaller because the acceptor also has a certain degree of rotational mobility, giving rise to additional randomization of mutual orientations. If the orientations of the donor and the acceptor are completely fixed, then one might expect rather large changes in the value of κ^2 and hence in the extent of energy transfer when their locations are switched. The fact that switching of the donor–acceptor locations has only small effects on either the extent of energy transfer or the trend of changes in energy transfer with respect to metal ion occupancy provides further justification for the choice of $\kappa^2 = {}^2/_3$.

Previously, Wang and Cheung (1984) have measured the distance between the same two residues in the binary TnC–TnI complex to be 50 Å in the presence of Ca^{2+} and 57 Å in its absence. Whereas our results show the same distance changes with respect to metal-binding states, our distances measured in the ternary complex are considerably smaller. This discrepancy may be due to a true difference in the geometry of the ternary versus the binary complex or to the fact that different acceptors were used in the two studies.

Dobrovol'sky et al. (1984) reported that Cys-98 of TnC and Cys-133 of TnI can be cross-linked by 1,3-difluoro-4,6-dinitrobenzene. More recently, we found that cross-linkers of various lengths can be used to cross-link the two residues and that a disulfide bond can be formed between them by using Nbs_2 as a catalyst (Park et al., 1988). Thus, both energy-transfer and cross-linking results are consistent with the picture that the protein regions containing the two cysteines possess considerable flexibility, so that the distance between them can take on variable values. The situation is reminiscent of the reactive sulfhydryls (SH_1 and SH_2) of myosin S1, which can also be cross-linked by a variety of reagents (Reisler et al., 1974; Wells et al., 1980; Wells & Yount, 1980), and energy-transfer studies (Dalbey et al., 1983; Cheung et al., 1985) using probes attached to these sulfhydryls seem to reveal a distribution of distances (Cheung et al., 1987).

Our findings may be relevant to the mechanism of thin filament regulation insofar as they provide evidence for a movement of the Cys-133 region of TnI toward the Cys-98 region of TnC upon binding of Ca^{2+} to the triggering sites of TnC. This movement may be coordinated with a movement of TnI away from actin as proposed in certain models for thin filament regulation (Hitchcock et al., 1973; Margossian & Cohen, 1973; Potter & Gergely, 1974) and recently demonstrated by Tao et al. (1987). Further work is underway to characterize this and other Ca^{2+}-induced distance changes in the thin filament.

Acknowledgments

We thank Dr. Enoch Small for the method-of-moments analysis program (FLUOR) and Drs. S. S. Lehrer and Z.

Grabarek for critically reviewing the manuscript.

Registry No. Cys, 52-90-4; Ca, 7440-70-2; Mg, 7439-95-4.

REFERENCES

Amir, D., & Haas, E. (1987) *Biochemistry 26*, 2162–2175.

Balint, M., Sreter, F. A., Wolf, I., Nagy, B., & Gergely, J. (1975) *J. Biol. Chem. 250*, 6168–6177.

Cheung, H. C., Gonsoulin, F., & Garland, F. (1985) *Biochim. Biophys. Acta 832*, 52–62.

Cheung, H. C., Johnson, M. L., Lakowicz, J. R., Joshi, N., & Gryczynski, I. (1987) *Biophys. J. 51*, 86a.

Chong, P. C. S., & Hodges, R. S. (1981) *J. Biol. Chem. 256*, 5071–5076.

Chong, P. C. S., & Hodges, R. S. (1982) *J. Biol. Chem. 257*, 2549–2555.

Dalbey, R. E., Weiel, J., & Yount, R. G. (1983) *Biochemistry 22*, 4696–4706.

Dalgarno, D. C., Grand, R. J. A., Levine, B. A., Moir, A. J. G., Scott, G. M. M., & Perry, S. V. (1982) *FEBS Lett. 150*, 54–58.

Dobrovol'sky, A. B., Gusev, N. B., & Friedrich, P. (1984) *Biochim. Biophys. Acta 789*, 144–151.

dos Remedios, C. G., Miki, M., & Barden, J. A. (1987) *J. Muscle Res. Cell Motil. 8*, 97–117.

Ebashi, S., & Endo, M. (1968) *Prog. Biophys. Mol. Biol. 18*, 123–183.

Fairclough, R. H., & Cantor, C. R. (1978) *Methods Enzymol. 28*, 347–379.

Grabarek, Z., Drabikowski, W., Leavis, P. C., Rosenfeld, S. S., & Gergely, J. (1981) *J. Biol. Chem. 256*, 13121–13127.

Grabarek, Z., Grabarek, J., Leavis, P. C., & Gergely, J. (1983) *J. Biol. Chem. 258*, 14098–14102.

Greaser, M. L., & Gergely, J. (1971) *J. Biol. Chem. 246*, 4226–4233.

Greaser, M. L., & Gergely, J. (1973) *J. Biol. Chem. 248*, 2125–2133.

Haas, E., Katchalsky-Katzir, E., & Steinberg, I. Z. (1978) *Biochemistry 17*, 5064–5070.

Haas, E. Wilchek, M., Katchalsky-Katzir, E., & Steinberg, I. Z. (1975) *Proc. Natl. Acad. Sci. U.S.A. 72*, 1807–1811.

Hartshorne, D. J., & Mueller, H. (1968) *Biochem. Biophys. Res. Commun. 31*, 647–653.

Hitchcock, S. E. (1975) *Eur. J. Biochem. 52*, 255–263.

Hitchcock, S. E., Huxley, H. E., & Szent-Györgyi, A. G. (1973) *J. Mol. Biol. 80*, 825–836.

Hudson, E. N., & Weber, G. (1976) *Biochemistry 15*, 672–680.

Johnson, J. D., Charlton, S. C., & Potter, J. D. (1979) *J. Biol. Chem. 254*, 3497–3502.

Kawato, S., Kinosita, K., Jr., & Ikegami, A. (1977) *Biochemistry 16*, 2319–2324.

Lakowicz, J. R., Gryczynski, I., Cheung, H. C., Wang, C.-K., & Johnson, M. L. (1988) *Biopolymers 27*, 821–830.

Leavis, P. C., & Gergely, J. (1984) *CRC Crit. Rev. Biochem. 16*, 235–305.

Leavis, P. C., Gowell, E., & Tao, T. (1984) *Biochemistry 23*, 4156–4161.

Leszyk, J., Collins, J. H., Leavis, P. C., & Tao, T. (1987) *Biochemistry 26*, 7042–7047.

Margossian, S. S., & Cohen, C. (1973) *J. Mol. Biol. 81*, 409–413.

Park, H.-S., Gong, B.-J., & Tao, T. (1988) *Biophys. J. 53*, 587a.

Perkins, W. J., Weiel, J., Grammer, J., & Yount, R. G. (1984) *J. Biol. Chem. 259*, 8786–8793.

Perry, S. V., Cole, H., Head, J. F., & Wilson, F. J. (1972) *Cold Spring Harbor Symp. Quant. Biol. 37*, 251–262.

Potter, J. D., & Gergely, J. (1974) *Biochemistry 13*, 2697–2703.

Potter, J. D., & Gergely, J. (1975) *J. Biol. Chem. 250*, 4628–4633.

Reisler, E., Burke, M., Himmelfarb, S., & Harrington, W. F. (1974) *Biochemistry 13*, 3837–3840.

Robertson, S. P., Johnson, J. D., & Potter, J. D. (1981) *Biophys. J. 34*, 559–569.

Schaub, M. C., & Perry, S. V. (1969) *Biochem. J. 115*, 993–1004.

Small, E., & Isenberg, I. (1976) *Biopolymers 15*, 1093–1100.

Spudich, J. A., & Watt, S. (1971) *J. Biol. Chem. 246*, 4866–4871.

Strasburg, G. M., Leavis, P. C., & Gergely, J. (1985) *J. Biol. Chem. 260*, 366–370.

Stryer, L. (1978) *Annu. Rev. Biochem. 47*, 819–846.

Tao, T., Lamkin, M. L., & Lehrer, S. S. (1983) *Biochemistry 22*, 3059–3066.

Tao, T., Gergely, J., & Leavis, P. C. (1986) *Biophys. J. 49*, 142–143.

Tao, T., Gong, B.-J., & Leavis, P. C. (1987) *Biophys. J. 51*, 27a.

Wang, C.-K., & Cheung, H. C. (1984) *J. Mol. Biol. 190*, 509–521.

Weeds, A. G., & Pope, B. (1977) *J. Mol. Biol. 111*, 129–157.

Weeks, R. A., & Perry, S. V. (1978) *Biochem. J. 173*, 449–457.

Wells, J. A., & Yount, R. G. (1980) *Biochemistry 19*, 1711–1717.

Wells, J. A., Knoeber, C., Sheldon, M. C., Werber, M. M., & Yount, R. G. (1980) *J. Biol. Chem. 255*, 11135–11140.

Zot, A. S., & Potter, J. D. (1987) *Annu. Rev. Biophys. Biophys. Chem. 16*, 535–559.